

# Predicting Threshold Entrainment Mass for a Boulder Beach

Mark S. Lorang

College of Oceanography and Atmospheric Sciences  
Oregon State University  
Corvallis, OR 97331, U.S.A

## ABSTRACT

LORANG, M.S., 2000. Predicting threshold entrainment mass for a boulder beach. *Journal of Coastal Research*, 16(2), 432-445. Royal Palm Beach (Florida), ISSN 0749-0208.



The critical threshold mass for boulders composing a beach is the mass of the largest stone entrained by the hydraulic forces associated with wave breaking and swash run-up. For any given storm event there is a maximum boulder mass that can be moved and another slightly larger boulder that has the minimum mass necessary to remain stable. Two equations are derived: one to estimate critical threshold mass and another to estimate minimum stable mass for boulders on a beach. The equations incorporate: stone density, beach slope, breaking wave height, water depth, wave period, run-up height, maximum swash velocity and average swash velocity. In both equations the wave force applied to the beach face is scaled relative to the elevation that wave energy raises the water surface. Scaling the wave force relative to the run-up elevation results in a critical threshold formula. This is given as equation (45). Its predictions accurately match field data giving the largest boulder transported on a beach during storm events. Scaling the wave force relative to the breaking wave height at the toe of the beach results in a stability formula. This is given as equation (46). It predicts stable mass in the range defined by the Hudson formula. Equation (46) has an advantage over the Hudson formula by incorporating the physically important parameters of wave period and swash velocity. Both equations could be useful in the initial evaluation and design of dynamic revetments constructed with quarry stone.

**ADDITIONAL INDEX WORDS:** *Wave runup, swash velocity, coastal engineering, dynamic revetment, gravel beach.*

## INTRODUCTION

### Boulder Beaches

Boulder beaches are common features of many rocky coasts throughout the world. They generally form at the base of sea cliffs and provide a protective buffer against wave attack. Natural boulder beaches deform in profile relative to changing storm wave conditions that transport boulders composing the beach. (OAK, 1981; 1985). OAK (1981) found that boulder entrainment occurred only during storms and that initial displacement was in direct response to wave breaking and up-rush of the wave swash. In this context, boulder beaches represent the natural equivalent to a dynamic rubble revetment. BAGNOLD (1940) argued that the potential energy carried away by the water that percolates into the beach results in a situation where the return flow of the backwash will be a less competent flow than the up-rush of the swash. The main role of the backwash on a boulder beach is to remove finer material, thereby maintaining an armored beach face characterized by high porosity. These dynamic characteristics of a boulder beach buffer the backshore environment from direct wave attack. The result is that sea cliffs, with boulder beaches developed at their toe, erode at very slow rates. Therefore, the ability to quantify the wave conditions necessary to initiate movement and transport of boulders is important for coastal engineers interested in the design of dy-

namic revetments that mimic the natural shore protection behavior of a boulder beach.

### Coastal Engineering Design

Over the last decade interest has turned towards the design of dynamic revetments that provide the necessary level of protection by allowing the structure to deform under wave attack (PILARCZYK and DER BOER, 1983; VAN DER MEER and PILARCZYK, 1986; JOHNSON, 1987; VAN DER MEER, 1987 and 1988; POWELL, 1988; AHRENS, 1981; LORANG, 1991; VAN DER MEER, 1992; SILVESTER and HSU, 1993). In this light, coastal engineers are designing with the intent to mimic the dynamic behavior of naturally occurring boulder, cobble and gravel beaches. However, an equation does not exist that estimates the critical threshold mass for use in the design of dynamic revetments.

The most frequently used formula for breakwater and static shoreline revetment design is the Iribarren formula (1938), modified by HUDSON (1952) and adopted as the Hudson formula by the Army Corps of Engineers in their *Shore Protection Manual* (SPM, 1984). The Hudson formula gives estimates of individual stone mass necessary to construct a static shore protection structure in terms of wave height, structure slope and stone density. It is given as

$$W = \frac{\rho_s H_s^3}{K_D \left( \frac{\rho_s - \rho_w}{\rho_w} \right)^3 \cot \theta} \quad (1)$$

where  $W$  is the minimum stable mass,  $H_s$  is the significant deep-water wave height or the significant wave height at the structure base,  $\rho_s$  and  $\rho_w$  are stone and water density, respectively,  $\theta$  is the angle the beach makes with the horizontal, and  $K_D$  is a stability coefficient empirically derived from wave tank studies (SPM, 1984). One can see from the equation that stone mass is mainly a function of the significant design wave height. Other wave parameters are ignored such as, wave period, swash velocity or run-up height. Unfortunately, these are the physical parameters that describe wave action upon a shoreline revetment designed to provide protection against wave erosion.

In the case of estimates from the Hudson formula, waves smaller than the design height can damage a coastal structure, ranging from the transport of a few individual stones to complete failure of the structure (AHRENS and McCARTNEY, 1975; BRUUN and GUNBAK, 1977; AHRENS, 1981). Such damage has been attributed in part to the effect wave period has on the hydraulic forces acting against a coastal structure (BRUUN and GUNBAK, 1977). An increase in wave period for any given wave height results in an increase in wave power expended on the structure. One would intuitively expect the corresponding entrainment of increasingly larger stones. The fact that wave period is not included in the Hudson formula has been cited as a shortcoming in its use as a design tool (HUDSON, 1952; BRUUN and GUNBAK, 1977).

The Army Corps of Engineers responded to this shortcoming in the theoretical development of the Hudson formula with numerous wave tank studies aimed at finding values for the stability coefficient,  $K_D$ , that accounted for stability through interlocking structure units or special placement of stones (HUDSON, 1952; SPM, 1984). When estimating stable stone mass, the typical design procedure is to consult the tables presented in the SPM and choose the proper  $K_D$  value that corresponds with the structure material, mode of placement, morphology (*i.e.* structure head or trunk) and the expected form of wave breaking. The Hudson formula has been a useful tool in the design of static structures because it relies on readily attainable variables that result in an over-estimate of minimum stable stone mass, thereby providing an adequate level of design safety. However, a similar formula does not exist for the design of dynamic revetments and the coastal engineer is left with having to estimate proper values for the stability coefficient,  $K_D$ , that reflect the critical threshold entrainment condition from the Hudson formula.

## ANALYSIS OF BOULDER ENTRAINMENT ON A BEACH

### Descriptive Processes

Wave competence is a term used here that refers to the size of the largest entrained boulder as related to the wave hydraulics that caused the entrainment. The entrainment of boulders on a boulder beach is viewed as occurring during two regimes of wave energy. The first is a relatively low-wave energy regime that occurs during periods of low-wave height and long-wave period. For this regime, only a small portion of the boulders comprising the beach are selectively entrained. The main processes would be (1) winnowing away of

fine material, (2) some boulder rounding due to impact fragmentation, and (3) some boulder smoothing due to abrasion. The second regime occurs at a higher energy level associated with storm wave conditions. This high energy regime is characterized by a dynamic beach state where most, or all, of the boulders shift position or rock in place, with the smaller boulders perhaps being rolled over or pushed up-slope.

One might argue that during storms wave breaking on the beach face dislodges individual boulders that are then pushed up-beach by the swash. BRUUN and GUNBAK (1977) found that as swash velocity increased, large over-turning moments developed on the blocks composing a quarry-stone structure. The result was the initial movement of individual stones. NOVAK (1969) measured the size of the largest transported clast on a gravel beach and the velocity of the swash. The largest gravel clast transported had an intermediate particle diameter of 0.1 m and was transported by a swash velocity of 2.42 m/s corresponding with a breaker height of 0.44 m. Therefore, swash velocity associated with small waves (0.44 m) can produce turbulent flow sufficiently competent to entrain both the gravel and cobble components of the beach. The conclusion from the above discussion is that swash velocity must be used in the development of a wave-competence equation.

The remainder of the discussion section of this paper is organized into six sequential sub-sections.

- nearshore wave transformation
- beach slope and swash deceleration
- swash resistance and beach roughness
- increasing wave power and wave competence
- Shields entrainment function applied to a boulder beach
- derivation of the two equations: one to estimate critical threshold mass and another to estimate minimum stable mass for boulders on a beach.

Each of these six sections describe how they relate to the derivation of the two equations (45) and (46) presented. I begin with a discussion of the methods used to estimate wave transformation from deep water to run-up of wave swash. Then a discussion of the relationship of beach slope and swash deceleration through the derivation of the Iribarren number,  $\xi$ , is presented. Similar arguments of beach slope and swash deceleration occurs in part because of flow resistance. Therefore, the assumptions and methods used to represent the drag coefficients that arise in the derivations are discussed in terms of beach roughness. The term wave competence, where the size of the largest entrained boulder reflects the wave hydraulics that caused the entrainment, is discussed through the relationship between increasing wave power and the entrainment of increasingly larger boulders. Finally, the derivation of the wave competence equations presented follow the derivation of the Shields entrainment function widely used to define threshold entrainment in the fluvial environment. Therefore, the derivation of the Shields entrainment function is briefly presented to highlight the derivation as applied to a boulder beach.

### Wave Transformations and Beach Scaling

The transformation from deep-water waves to final run-up,  $R_w$ , of wave swash on the beach face is a complex process that

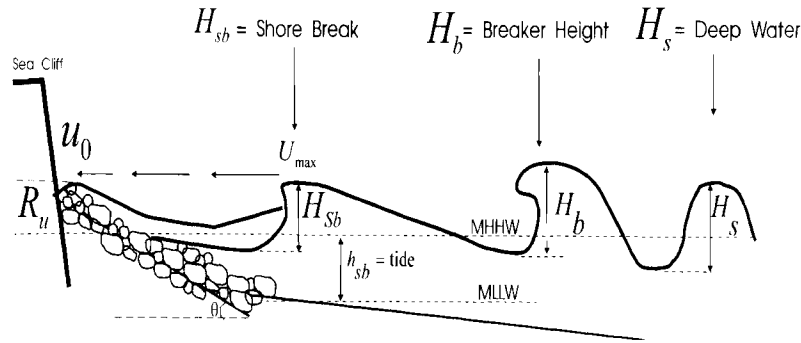


Figure 1. Schematic of the process of wave transformation from an initial off-shore wave height to the final run-up of swash on the beach face.

becomes increasingly so for a low sloping nearshore. As storm energy increases incident waves continually break further offshore producing a surf zone 100's of meters wide on low sloping sand beaches or broad wave cut terraces. These surf zones may have many bores between the break-point and final run-up. On many gravel, cobble and boulder beaches storm waves never reach the beach face during low tide. The energy is dissipated in the wide surf zone over the wave-cut terrace that exists at that tide level. In contrast, during high tide, and under similar storm intensity, waves initially break very near the beach face separated by maybe one or two surf bores (Figure 1). Estimating run-up elevation from offshore wave conditions is most reliable when wave breaking occurs close to the beach without a large intervening surf zone.

Wave run-up can be estimated from the deep-water wave statistics and slope of the beach. BATTJES (1974; a & b) modified the HUNT (1959) formula for the 2% run-up elevation,  $R_{u2\%}$ , by re-writing the equation in terms of a dimensionless surf similarity parameter,  $\xi$ , that he referred to as the Iribarren number. The expression

$$R_{u2\%} = C_r H_s \xi \tag{2}$$

relates the run-up elevation to the Iribarren number,  $\xi$ , the deep-water significant height,  $H_s$ , and an empirical constant  $C_r$ . The Iribarren number is a non-dimensional parameter that relates beach steepness to offshore wave steepness. It is an important scaling parameter when estimating run-up on a boulder beach or similar artificial rock slopes (BATTJES, 1974; a & b; AHRENS and MCCARTNEY, 1975; AHRENS, 1981; ALLSOP *et al.*, 1985; HOLMAN, 1986; DALRYMPLE, 1992; WAAL and VAN DER MEER, 1992; VAN DER MEER and STAM, 1992). The expression is

$$\xi = \frac{\tan \theta}{\sqrt{\frac{H_s}{L_0}}} \tag{3}$$

where  $\tan \theta$  is the slope of the beach and  $L_0$  is the deep-water wave length. From linear wave theory we can derive an approximation for  $L_0$ , given as

$$L_0 = \frac{1}{2\pi} g T^2 \tag{4}$$

where  $T$  is the wave period and  $g$  is gravity. Substitution of (4) into (3) and (3) into (2) yields

$$R_{u2\%} = C_r \sqrt{\frac{g}{2\pi}} T \sqrt{H_s} (\tan \theta). \tag{5}$$

VAN DER MEER and STAM (1992) found a value of 0.55 for  $C_r$ , corresponding to a range of  $0.5 > \xi < 2$  due to irregular waves on porous rock slopes. They referred to  $C_r$  as the run-up attenuation constant and found that it depends on beach coarseness and permeability which attenuates the run-up through frictional resistance of the swash and loss of water. HOLMAN (1986) also found similar values for  $C_r$  using measures of swash from a sand beach. For very steep boulder beaches as wave energy increases run-up elevation increases in a linear fashion at incident wave frequencies for the range of surf similarity parameters  $0.5 > \xi < 2.5$  (HOLMAN, 1986; KOBAYASHI, *et al.* 1988; VAN DER MEER and STAM, 1992). The data used here come from storm conditions where  $\xi$  fell within this range (Table 1). Gravel and boulder beaches typically exist in this range for  $\xi$ . The fundamental physical principles between beach slope and wave steepness are related through the derivation of  $\xi$ . Therefore, the derivation follows below illustrating how those arguments can be used to derive the wave competence equations presented here.

We begin with a wave impinging on a gravel or boulder slope as a swash bore that collapses at the shore break and surges up the gravel beach face (Figure 1). This swash bore must decelerate from a maximum velocity,  $u_{max}$ , at the shore break position (equal to maximum run-down for monochromatic waves) to zero over a time interval ideally equal to  $\frac{1}{2}$  the wave period. We can approximate maximum velocity with the following

$$u_{max} = \sqrt{g H_{sb}} \tag{6}$$

where  $H_{sb}$  is the wave height at the shore break position. We can define a time interval  $t$  as

$$t = \frac{T}{2}. \tag{7}$$

The deceleration,  $\partial u / \partial t$  of the swash equals the down slope component of gravity,  $g \sin \theta$ . This condition written for a sloping beach is

Table 1. Oak (1985) data and other variables estimated by the listed equation number.

Oak Data			Supplemental Analysis				
$H_s$ Buoy (m)	$T$ Buoy (sec)	Largest Boulder (kg)	$\zeta$ (3) (ND)	$H_b$ (50) (m)	$R_{u2/3}$ (5) (m)	$U_{max}$ (30) (m/s)	Crit. Thr (48) (kg)
2.1	10	28	1.35	2.8	1.56	7.91	195
2.2	12	53	1.59	3.12	1.92	8.36	318
2.2	11	93	1.45	3.02	1.76	8.22	262
2.3	11	24	1.42	3.12	1.8	8.36	285
3.2	12	27	1.32	4.21	2.32	9.71	647
3.3	11	39	1.19	4.17	2.16	9.66	567
4.2	14	24	1.34	5.57	3.1	11.17	1523
4.3	14	2191	1.32	5.68	3.13	11.27	1593
5.1	15	898	1.30	6.69	3.65	12.24	2563
5.4	11	1276	0.93	6.19	2.76	11.77	1444
6	12	935	0.96	6.97	3.17	12.49	2137

$$\frac{\partial u}{\partial t} = g \sin \theta \tag{8}$$

where  $\theta$  is the angle between the beach face and horizontal (Fig. 1). We can now make the following approximation through substitution

$$\frac{\partial u}{\partial t} \approx \frac{\sqrt{gH_s}}{0.5T} = g \sin \theta \tag{9}$$

where the substitution of  $H_s$  for  $H_{sb}$  is required to equate offshore wave steepness to beach slope as expressed in the Iribarren number. Solving for  $\sin \theta$  and squaring both sides yields

$$(\sin \theta)^2 = \frac{H_s}{0.25gT^2} \tag{10}$$

solving (4) for wave period yields

$$T^2 = L_0 \left( \frac{2\pi}{g} \right) \tag{11}$$

and substituting (11) into (10) yields

$$(\sin \theta)^2 = \frac{H_s}{0.25g \left( L_0 \frac{2\pi}{g} \right)} \tag{12}$$

squaring both sides and rearranging as a ratio equal to some constant yields

$$\frac{\sin \theta}{\sqrt{\frac{H_s}{L_0}}} = \text{constant} = \xi \tag{13}$$

where the constant is the Iribarren number,  $\xi$ , related to wave steepness and beach slope expressed as  $\sin \theta$ .

### Beach Roughness and Swash Resistance

Swash deceleration on the beach face occurs in part because of flow resistance caused by roughness. Flow resistance, in a river, occurs in part because of bed roughness associated with particle size. Maximum roughness for a river channel occurs when particle diameter approaches flow depth

(VAN RIJN, 1982). Analogously, on a boulder beach, flow resistance of the swash up the beach face occurs in part due to the roughness associated with boulder size. The condition of maximum roughness occurs when boulder diameter equals run-up,  $R_u$ , or when the swash thickness equals the boulder diameter (Figure 2). This type of roughness scale becomes important when estimating the frictional drag between the beach face and the swash. The ratio used here to express average roughness of a boulder beach is

$$\frac{R_u}{D_{50}} \tag{14}$$

where  $D_{50}$  is the mean intermediate diameter of the boulder comprising the beach face.

HUGHES (1995) presents an equation for estimating the frictional resistance,  $f_r$ , associated with wave swash up a low sloping sand beach face

$$f_r = \frac{8}{\left( 2.5 \ln \left( 30 \frac{h_s}{k_s} \right) \right)^2} \tag{15}$$

where  $h_s$  is the thickness of the swash at any point on the beach face and  $k_s$  relates to grain size. This expression is derived from arguments of boundary layer thickness for fully turbulent flow. HUGHES (1995) made the assumption that swash velocity on a low sloping sand beach can be approximated as steady flow and noted that the roughness ratio,  $h_s/k_s$ , should be adjusted to account for friction caused by entrained sediment. Similarly, an assumption is made that roughness scaled by the run-up height and boulder size modifies equation (15) into a first-order expression for the frictional resistance,  $f_{BF}$ , between the swash and surface of a boulder beach. This is done through substitution of equation (14) for the roughness ratio,  $h_s/k_s$ , in equation (15) and also assuming that  $f_r$  is proportional to  $f_{BF}$ , thus yielding

$$f_{BF} = \frac{8}{\left( 2.5 \ln \left( 30 \frac{R_u}{D_{50}} \right) \right)^2} \tag{16}$$

Wave tank experiments have shown that frictional drag of

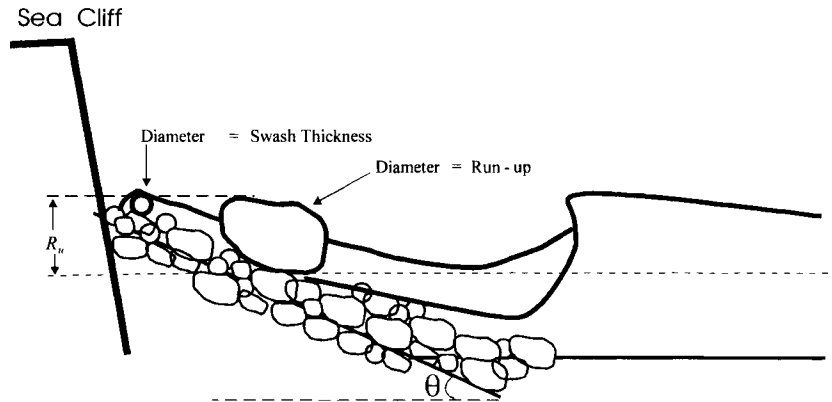


Figure 2. Schematic diagram for two conditions of maximum roughness; one when boulder diameter equals run-up elevation and another when boulder diameter just equals swash thickness.

wave swash ranges from 0.3 for rough angular rip rap to 0.05 or less for smooth cobble and boulder slopes (KOBAYASHI and GREENWALD, 1986; KOBAYASHI, *et al.*, 1988; KOBAYASHI and DESILVA, 1989). Under maximum roughness conditions, where  $R_u = D_{50}$ , equation (16) gives a maximum value of 0.1 for  $f_{BF}$ . Data used from an Australian boulder beach gives an average value of 0.03 for  $f_{BF}$  with equation (16). This value is consistent with reported values from experimental work. Equation (16) is used simply as an objective way of determining a value for the drag coefficient,  $f_{BF}$ , that appears in the derivation of wave stress applied the beach face due to wave breaking and swash run-up. Improvements in the predictions from the critical threshold and stability equations derived would be expected given a better means of expressing frictional resistance. However, equation (16) does give an objective estimate of frictional resistance within an expected range of published values and by using easily obtainable physical data. Therefore, it represents a best estimate at this time.

### Wave Power and Wave Competence

The ability of waves to entrain boulders is referred to as wave competence and should be related to the available wave power. Wave power is the flux of energy available to entrain boulders composing a steep sloping beach. It is intuitive that as wave power increases during storms that correspondingly larger boulders will be mobilized. Wave power,  $P_o$ , is the shoreward flux of wave energy and in deep water is written as

$$P_o = EC_g n \quad (17)$$

where  $E$  is wave energy,  $C_g$  is the group velocity and  $n$  is a dimensionless coefficient that varies with depth. It is equal to 0.5 in deep water and increases to 1 as the wave shoals to the break point (KOMAR, 1998). Wave energy,  $E$ , can be written as

$$E = \frac{1}{8} \rho_w g H_s^2 \quad (18)$$

and the group velocity,  $C_g$ , is given as

$$C_g = (g/4\pi)T \quad (19)$$

From these expressions one can see that wave power,  $P_o$ , can be written as

$$P_o = \text{constant} \cdot H_s^2 T \quad (20)$$

Both wave period and power are conservative properties, hence wave height must increase in equation (20) during the process of shoaling from deep water to the initial break point, which is what one physically observes. The point being illustrated here is that increasing the wave period for any given wave height will increase the wave power (equation 20) available to mobilize boulders on a beach. Therefore, a wave competence equation should reflect a wave period dependence where an increase in wave power should be related to a corresponding increase in predicted wave competence.

Swash velocity is also important for threshold entrainment. However, the movement of boulders during storms occurs in response to other hydraulic complexities associated with wave breaking and swash run-up. These complexities arise from factors such as: dynamic pressure forces directly related to breaking waves, flow deceleration of the swash, and internal head pressure within the beach matrix due to percolation.

The approach taken here is that the hydraulic forces active during storms are best represented by the wave height at the shore break position,  $H_{sb}$ , wave period,  $T$ , run-up elevation of the wave swash,  $R_u$ , and estimates of maximum and average swash velocities,  $U_{max}$  and  $U_{avg}$ , respectively (Figure 3). The height of the breaker directly impinging the beach face,  $H_{sb}$ , is analogous to engineering specifications that require determining wave height at the base of the structure. Wave height at the shore break,  $H_{sb}$ , is depth dependent and maximum heights can be estimated from the tide elevation above mean low water level. This is possible given that the toe of a boulder or gravel beach typically coincides with elevation of the low tide terrace (NICHOLS, 1988 and 1990). A wave-cut, low-tide terrace provides the necessary support for the boulder and gravel beach material to rest upon.

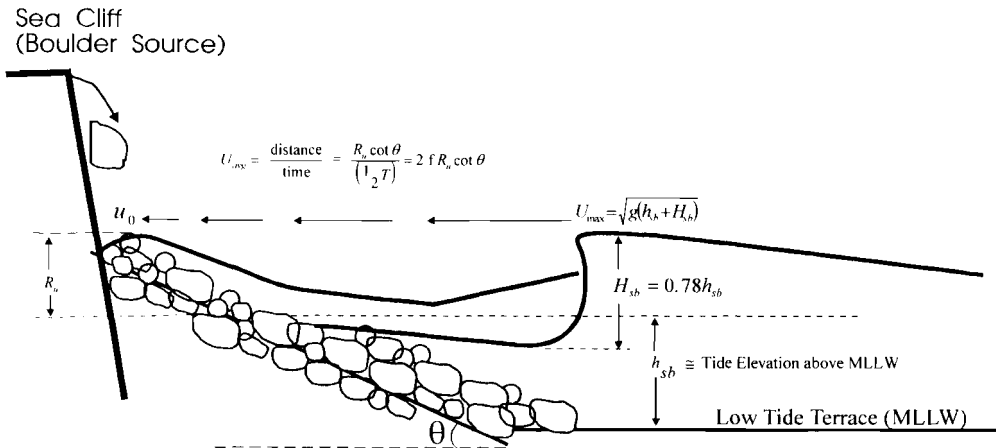


Figure 3. Schematic depiction of wave collapse at the shore break position followed by swash run-up on a boulder beach showing variables used to determine boulder entrainment and stability. The low tide terrace typically corresponds to the mean low tide level given here as mean lower low water (MLLW) for a mixed semidiurnal tide.

**Threshold Entrainment and the Shields Entrainment Function**

For unidirectional flow, threshold entrainment occurs when the fluid force applied to the exposed surface area of a particle exceeds the particle's immersed weight. The size of the largest particle entrained is then a measure of the competence level of the mean flow to transport sediment. This concept of flow competence can be used to express shear stress as a function of particle diameter,  $D$ , of a sphere. It is derived from a force balance relation between the immersed weight force and the fluid drag force (Figure 4).

The immersed weight force,  $F_{iwt}$ , is the weight force in air minus the buoyant force when fully submerged and is given as

$$F_{iwt} = (\rho_s - \rho_w)g(\alpha_1 \cdot D^3) \tag{21}$$

where  $\rho_s$  is the density of the particle being entrained and  $\alpha_1$  is shape factor that relates to the particle volume (e.g.  $\pi/6$  for a sphere). The fluid drag force,  $F_d$ , can be written in the following manner

$$F_d = \tau \cdot D^2 \left( \frac{\alpha_2}{C_p} \right) \tag{22}$$

where  $C_p$  is a packing coefficient and  $\alpha_2$  is a shape factor (e.g.  $\pi/4$  for a circle). The ratio  $\alpha_2/C_p$  describes the projection surface area exposed to the flow dependent on the size, shape and packing arrangements of particles composing the river bed.

Critical threshold entrainment occurs when the moment of the drag force,  $F_d$ , about the pivot point C (Figure 4) equals the moment of the immersed weight force,  $F_{iwt}$

$$F_{iwt} \cdot \overline{AC} = F_d \cdot \overline{BC} \tag{23}$$

where

$$\overline{AC} = \left( \frac{D}{2} \sin \phi \right) \text{ and } \overline{BC} = \left( \frac{D}{2} \cos \phi \right) \tag{24}$$

and  $\phi$  is the pivoting angle (Figure 4).

Substitution of (24) into (23) and solving for the coefficients yields

$$C_p \frac{\alpha_1}{\alpha_2} \tan \phi = \frac{\tau_{crit}}{(\rho_s - \rho_w)gD} = \theta_{crit} \tag{25}$$

where  $\tau_{crit}$  is the critical shear stress at which threshold entrainment occurs and  $\theta_{crit}$  is a non-dimensional variable dependent on the distributions of particle size, shape and the packing of the bed. This dimensionless form of the critical shear stress is termed the Shields entrainment function.

The derivation of the wave competence equation below follows the same principles as the derivation of the Shields entrainment function above, the main difference being the way

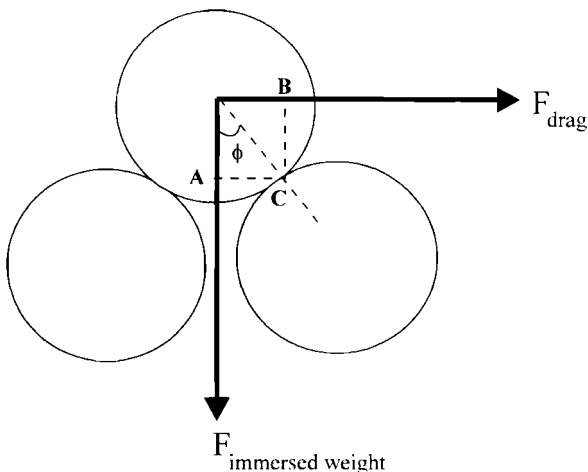


Figure 4. Schematic depicting the relationship between a drag force associated with a flowing fluid and a weight force acting on a sphere. The angle  $\phi$  reflects the pivoting angle between spheres about the contact point C and is affected by channel slope.

in which the expression for stress,  $\tau$ , is defined for a beach face.

## FORMULA DERIVATION

### Defining Stress on the Beach Face

For any environment the fluid force acting on a potentially mobile bed is the first quantity of interest when evaluating threshold entrainment. For a steady-state turbulent flow the boundary shear stress,  $\tau$ , is proportional to the fluid density and the square of the mean velocity  $U$ :

$$\tau \propto \rho_w U^2 \quad (26)$$

(HENDERSON, 1966; STERNBERG, 1972; YALIN and KARAHAN, 1979). Shear stress between a uniform turbulent flow and a potentially mobile bed can be derived from arguments of conservation of momentum yielding

$$\tau = f_r \rho_w U^2 \quad (27)$$

where  $f_r$  is a friction coefficient that refers to flow drag associated with bed roughness as water flows through a channel. This expression relates the time-averaged mean velocity near the bed to the force exerted by the fluid.

Wave swash up the beach face is not a steady flow but rather is a decelerating flow. Therefore, in order to apply equation (27) a modification for deceleration is needed. The first step is to separate and define two velocity terms; the maximum swash velocity,  $U_{max}$ , and the average swash velocity,  $U_{avg}$ . The second step is to substitute them into an expression for fluid stress more representative of the non-steady flow conditions of wave swash.

The maximum swash velocity,  $U_{max}$ , in shallow water is equal to the wave velocity at the shore break and is related to the depth of water,  $h_{sb}$ , plus the breaking wave height,  $H_{sb}$ , in the following manner

$$U_{max} = \sqrt{g \cdot (h_{sb} + H_{sb})}. \quad (28)$$

Ideally, swash velocity decreases from this maximum at the break point to zero at the maximum run-up elevation,  $R_u$  (Figure 3). Over the intervening distance, water percolates into the beach matrix as the swash momentum decreases resulting in a seaward flowing backwash after complete run-up.

The average swash velocity,  $U_{avg}$ , is used to represent swash deceleration as a function of wave period and beach slope. This is done by dividing the horizontal excursion distance of the run-up by the time it takes the swash to decelerate across that distance in a similar manner seen above in the derivation of the Iribarren number,  $\xi$ , (Figure 3). This deceleration occurs over a time period,  $t$ , ideally equal to  $\frac{1}{2}$  of the wave period,  $T$ , and the horizontal excursion distance,  $X$ , is defined by the run-up elevation and beach slope geometrically as

$$X = R_u \cdot \cot \theta. \quad (29)$$

The average velocity follows from substitution as

$$U_{avg} = \frac{X}{t} = \frac{R_u \cot \theta}{\left(\frac{1}{2}T\right)} = R_u 2f \cot \theta \quad (30)$$

where,  $f = 1/T$  is the swash frequency.

Equation (27) can be used as a starting point to make a first-order approximation of fluid stress applied to the beach face,  $\tau_{BF}$ , by substituting the product of maximum swash velocity,  $U_{max}$ , and the average velocity,  $U_{avg}$ , of the run-up for  $U^2$  in the following manner

$$\tau_{BF} = f_{BF} \rho_w |U_{max}| |U_{avg}| \quad (31)$$

where  $f_{BF}$  represents flow drag between the beach face and the wave swash (equation 16). This approach treats wave stress applied to the beach face by wave swash as a function of the wave period, maximum and average swash velocities, run-up elevation, and slope. Substitution of equation (28) and equation (30) into equation (31) yields

$$\tau_{BF} = f_{BF} \rho_w U_{max} R_u 2f \cot \theta \quad (32)$$

where  $\tau_{BF}$  is dimensionally consistent with  $\tau$ , equation (27).

In contrast with a river, the non-steady flow condition that characterizes the beach environment is addressed by separating the velocity squared term in (equation 27) into two components,  $U_{max}$ , and  $U_{avg}$ . The assumption is made that the  $U_{max}$  term represents the initial turbulent portion of wave uprush that gives the swash its initial momentum to travel up the beach face. The  $U_{avg}$  term represents the "energy-depletion" portion of the turbulent flow of wave swash up the beach face. During this phase the flow velocity of the swash decelerates in response to gravity, frictional resistance due to surface roughness and momentum lost to percolation. This aspect of swash deceleration enters the derivation through the dependence of  $U_{avg}$  on run-up elevation, beach slope and swash frequency (equation 30). Expressing wave stress in this manner modifies the steady-state turbulent flow expression (equation 27) into a non-steady expression (equation 32) applicable to at least first-order for wave stress applied to the beach face. The assumptions made above incorporate how far wave swash runs up the beach versus how long it takes to get there (equation 30), into a dimensionally correct expression for wave stress between the swash and the beach face (equation 32).

### Force Balance Considerations

The immersed weight of each boulder,  $F_{iwt}$ , is the force that holds it to the beach against the wave forces associated with wave collapse and swash run-up (Figure 5). The maximum boulder mass,  $m$ , that can be entrained by the wave force comes from the definition of the immersed weight force,  $F_{iwt}$ , in the following manner

$$F_{iwt} = (\rho_s - \rho_w) g \frac{m}{\rho_s}. \quad (33)$$

The flow trajectories of the water comprising the wave are initially directed into the beach and then forced in the up slope direction as wave swash. Likewise, the force of the wave initially tries to push the boulders horizontally in the direc-

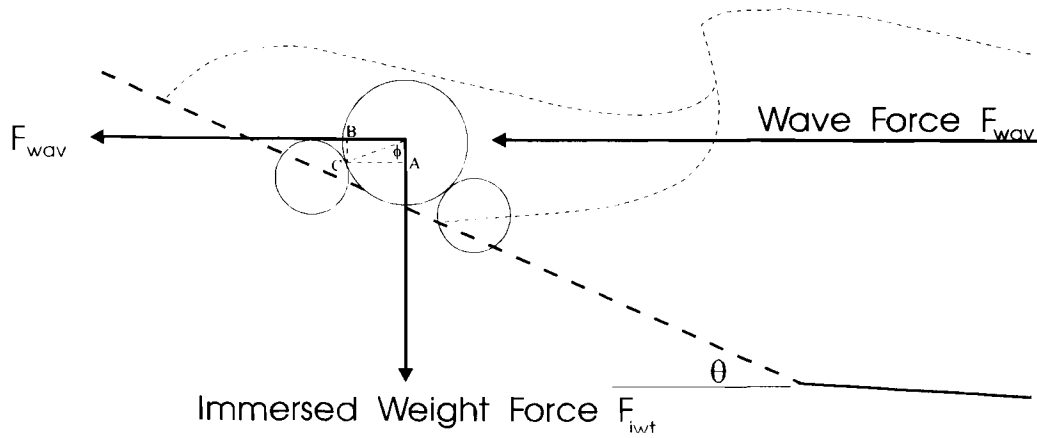


Figure 5. Schematic depicting the relationship between the wave force,  $F_{wav}$ , trying to push a spherical boulder into the beach and the weight force,  $F_{iwt}$ , acting to hold the boulder in place. The angle  $\phi$  reflects the pivoting angle with a nearly spherical boulder about the contact point C.

tion of wave propagation; however, entrainment occurs with the swash in the up-beach direction (Figure 5). To describe this relationship, the scalar value of the entraining wave force can be expressed as

$$|F_{wav}| = \tau_{BF} \cdot l^2 \tag{34}$$

where  $l$  is a length scale. An assumption is made that  $l^2$  corresponds to a vertical projection area of the beach face exposed to the available wave energy, rather than the surface area of an individual boulder.

The overall goal is to relate increased wave energy or power to the entrainment of larger boulders. This wave competence argument requires that the total wave force be scaled according to some factor related to wave energy. Maximum wave energy at the shore break is expressed as

$$E_{H_{sb}} = \frac{1}{8} \rho_w g H_{sb}^2 \tag{35}$$

and the remaining energy on the beach face can be approximated by the run-up elevation in the following manner

$$E_{R_u} = \frac{1}{8} \rho_w g R_u^2 \tag{36}$$

For the condition of critical threshold entrainment, the projection surface area of the beach exposed to the available wave energy is scaled by defining  $l$  equal to  $R_u$  resulting in

$$|F_{wav}| = \tau_{BF} \cdot R_u^2 \tag{37}$$

and substitution of equation (32) into equation (37) yields

$$|F_{wav}| = f_{BF} \rho_w U_{max} R_u^3 2f \cot \theta \tag{38}$$

Substitution of the run-up elevation,  $R_u$ , for  $l$  in equation (34) appropriately scales the wave force relative to the available wave energy. The result of scaling in this manner is that the wave force increases with increasing wave energy. Consequently, the final wave competence equation derived below predicts entrainment of increasingly larger boulders with increasing wave energy. This desired result would not occur if

the wave force was scaled relative to the surface area of a boulder. Therefore, scaling the wave force relative to the elevation that the wave energy raises the water surface,  $R_u$ , is a necessary first order assumption. Boulder surface area is included in the equation as part of the shape and packing coefficients in the derivation below (equation 42). Further development of a critical threshold entrainment equation for boulders on a beach follows that of the Shields entrainment function for critical threshold entrainment in rivers derived earlier.

### Critical Threshold Entrainment

Critical threshold entrainment for any boulder on the beach face occurs when the moment of the wave force,  $F_{wav}$ , about the pivot point C equals the moment of the weight force,  $F_{wt}$ ,

$$F_{wt} \cdot \overline{AC} = |F_{wav}| \cdot \overline{BC} \tag{39}$$

(Figure 5). Ideally the wave force only acts against the exposed projected surface area of the boulder, which is a function of size, shape and packing arrangements of the boulders composing the beach. Therefore, the wave force of equation (38) can be modified to account for these factors in the following manner

$$|F_{wav}| = \tau_{BF} \cdot R_u^2 \cdot \left( \frac{\alpha_1}{C_p} \right) \tag{40}$$

where  $\alpha_1$  is a shape factor and  $C_p$  is a packing coefficient that together describe the projection surface area exposed to the wave force. Critical threshold entrainment occurs when the wave force equals the weight force

$$F_{wt} = |F_{wav}| \tag{41}$$

Substitution of equation (33) for the immersed weight force and (40) for the wave force into the force balance expression (equation 41) and solving for the coefficients yields



$$\frac{C_p}{\alpha_1} \tan \phi = \frac{\rho_s \tau_{BF} R_u^2}{(\rho_s - \rho_w) g m}. \quad (42)$$

We can let

$$\frac{C_p}{\alpha_1} \tan \phi = K_r \quad (43)$$

where  $K_r$  is a non-dimensional variable. The product of the pivoting relationship,  $\tan \phi$ , between boulders and ratio of the packing coefficient to the shape factor forms a non-dimensional variable  $K_r$ , dependent on the distribution of boulder size, shape and the arrangement of boulders within the beach. This variable can be thought of as a complex constant related to interlocking nature of individual boulders and the overall stability of the beach matrix. This is analogous to the Shields entrainment function,  $\theta_{crit}$ , as well as the stability coefficient,  $K_D$ , in the Hudson Formula (1).

Friction and boulder interlocking are factors that oppose entrainment due to lift and drag forces and dynamic pressure forces that develop through wave breaking directly on the beach face and swash run-up. It may be possible to write even more complex equations that consider all of the possible force vectors associated with wave breaking and swash run-up. However, drag and lift forces depend on depth and velocity, both of which change across the beach face during wave run-up, as well as from wave to wave. The dynamic pressure forces depend on breaking wave form. Furthermore, all of these forces act upon boulder surface area that depends on size, shape, and packing arrangements of the boulders within the beach. Therefore, it is clearly evident that it would be extremely difficult at best to transfer a force vector analysis to a boulder beach exposed to a variable wave and tide climate and also composed of a distribution of boulder sizes and shapes (Figure 3). Moreover, it would be entirely impractical if not impossible to measure in the field the projection surface area, pivoting angles and interlocking relationships for all boulders composing a beach. Therefore, friction and interlocking are accounted for with the stability coefficient,  $K_r$ , in an analogous manner to the stability coefficient,  $K_D$ , of the Hudson Formula and the wave force is presented as a scalar related to wave energy through the substitution of run-up height for the length scale in equation (34).

The mass,  $m$ , of the largest boulder that can be entrained relative to the given wave force is the quantity of interest. Therefore, substitution of equation (43) into (42) and solving for mass,  $m$ , yields

$$m = \frac{\rho_s \tau_{BF} R_u^2}{K_r (\rho_s - \rho_w) g}. \quad (44)$$

and substitution of  $\tau_{BF}$ , equation (32), into (44) yields

$$M_{R_u} = \frac{\rho_s f_{BF} U_{max} R_u^3 2f}{K_r \left( \frac{\rho_s - \rho_w}{\rho_w} \right) g \tan \theta} \quad (45)$$

where  $M_{R_u} = m$  and refers to the critical threshold mass scaled relative to the run-up elevation. This represents the final form of the wave-competency equation. Equation (45) can be thought of as a threshold entrainment equation be-

cause, as will be shown, it estimates the critical threshold condition of boulder transport on a beach during storms.

One would expect that a slightly larger boulder would have the minimum mass necessary to remain stable. Substitution of the shore break wave height,  $H_{sb}$ , for  $l$  in equation (34) yields

$$M_{H_{sb}} = \frac{\rho_s f_{BF} U_{max} R_u H_{sb}^2 2f}{K_r \left( \frac{\rho_s - \rho_w}{\rho_w} \right) g \tan \theta}. \quad (46)$$

Here  $M_{H_{sb}}$  represents a boulder mass slightly larger than the predicted threshold entrainment mass,  $M_{R_u}$ , because it is scaled to a higher wave energy. Equation (46) is taken as the minimum mass necessary to maintain stability under the given wave conditions. This expression includes both the wave period and the swash velocity. It is compared with the Hudson formula (1) to illustrate that the mass estimates relate best to static conditions.

## FORMULA TESTING AND DISCUSSION

### The Data

Field data are used to compare estimates of boulder mass with equation (45). This data set comes from a field study where boulder transport on a beach was monitored over a two year period with wave heights and periods recorded by a nearby wave-buoy (OAK, 1985). A range of wave heights and periods are used to further demonstrate the effect of wave period and as a comparison of the stability equation (46) with the Hudson formula (1). This analysis compares significant offshore wave height  $H_s$  ranging from 1 m to 8 m on 0.5 m intervals and periods of 5, 10, and 15 seconds, respectively. The combination of wave heights and periods covers a range of natural possibilities.

Breaker heights, maximum and average swash velocity, and run-up heights are estimated from the significant deep water wave height,  $H_s$  and period,  $T$  and the slope of the beach face. Breaker height,  $H_b$ , was found using  $H_s$  and  $T$  with the following empirical expression given by KOMAR and GAUGHAN (1973)

$$H_b = 0.39g^{1/5}(T \cdot H_s^2)^{2/5}. \quad (47)$$

The stability coefficient  $K_r$  was set to one in an attempt to quantify how well the physical variables estimate field data. It is also noted that for smooth round cobbles the stability coefficient,  $K_D$ , of the Hudson formula was found from empirical wave tank data to be equal to a value of 1.2 and one would not expect these stability coefficients to differ greatly.

### Kiama Beach Field Data

Kiama Beach is a pocket beach on the South Western coast of Australia. It is 150 m long, 23 m wide with an average slope 0.157 (OAK, 1981). Cliff headlands supply boulder material for the beach that forms a boulder bank throughout the tidal zone with a mean size of 0.256 m (OAK, 1981). OAK (1981) monitored the movement of individual boulders from Kiama Beach for a period of two years. The movement of boulders was monitored by establishing a survey grid over

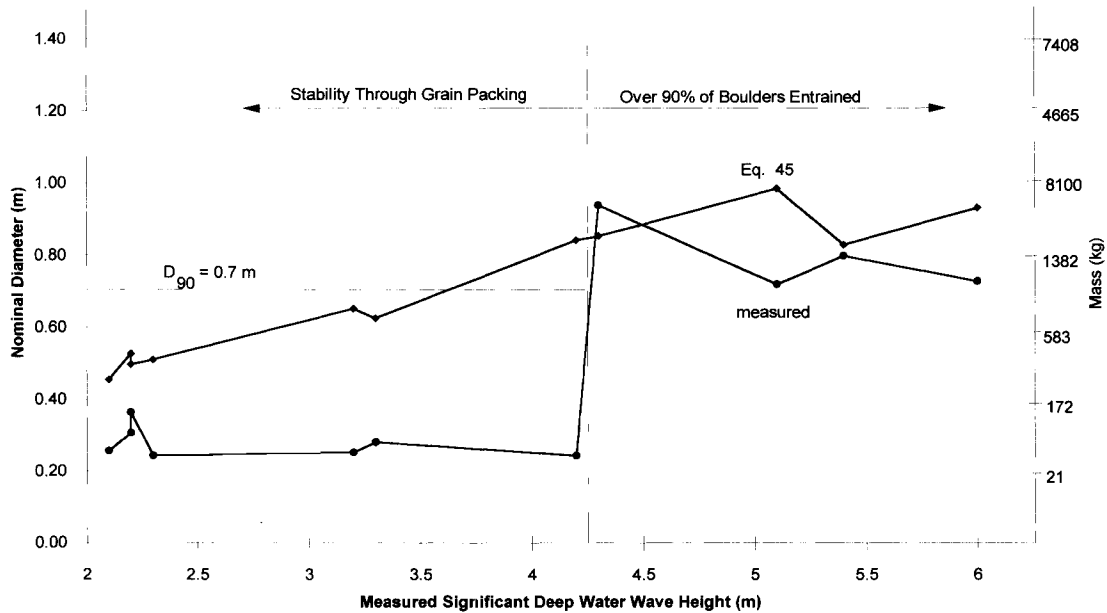


Figure 6. Comparison between threshold equation (45) and field data of Oak (1985). The nominal diameter is the diameter of a sphere of equal mass and is included to give a better understanding of the size of the boulders relative to the mass.

the beach and recording the position and size of individual boulders corresponding to each grid point. During the monitoring period Kiama beach was surveyed eleven times following the passing of storms. Wave heights and periods were recorded from a local offshore wave-buoy. The mass of the largest boulder that had been moved by waves was also recorded. These data were published in OAK (1985) and are arranged here in the first three columns of Table 1 in order of increasing wave height of each storm event. The values for the Iribarren number,  $\xi$ , for each reported storm event fell within the range appropriate for estimates of run-up height with equation (5) (Table 1). Those values are used to compare both equations (45) and (46) and the field data of OAK (1985). The value of  $\rho_s$  was estimated at  $2700 \text{ kg/m}^3$  and the value for stability coefficient,  $K_D$ , was taken as 1.2. Values for the stability coefficient,  $K_D$ , range from a low value of 1.2 for smooth rounded cobbles to 7 for placed angular stone (Table 7–8, SPM 1984). For the Hudson formula larger values of  $K_D$  reflect the increased collective strength gained due to interlocking of the placed angular rock.

#### Critical Threshold Equation (45) versus Field Data

The critical threshold equation (45) adequately approximates (within a factor of 2 to 3) boulder mass at low wave heights of 2 m or less and gives better estimates (less than a factor of 2) at wave heights above 4.25 m (Figure 6). The drop in estimated mass for an increase in wave height of 5.1 m and 5.4 m is due to a respective decrease in wave period from 15 to 11 seconds (Figure 6 and Table 1). This illustrates that increasing wave power also increases the size of boulders that can be transported, confirming the intuitive expectations that lead to the derivation of both equations (45) and (46).

The poor correlation between equation (45) and field data for wave heights less than 4 m is interpreted as due to interlocking and friction between particles dominating the hydraulic forces (Figure 6). The friction between particles would be related to size, shape, and packing of the boulders composing Kiama Beach. From this perspective equation (45) can only predict the potential maximum entrainment size for low wave conditions where grain to grain interlocking of a mixed bed dominates applied wave forces. This is the same paradox found in flow competence evaluations for gravel bed rivers and can only be addressed through empirical evaluations of site specific conditions. The value for  $K_r$  would have to increase to reflect the interlocking nature of a packed, mixed size and shape beach matrix. The value of the  $K_D$  coefficient for the Hudson formula increases from 1.2 to 7 to reflect increased interlocking due to special placement of stones.

OAK (1981) made a plot of wave-buoy data over the beach monitoring period that showed wave heights of 2 m having an approximate 50% exceedance probability, and waves of 4 m a 2% exceedance probability. Storm wave conditions (wave heights > 4 m) are competent to transport the mean boulder size of 0.25 m (Figure 6). The  $D_{90}$  boulder size for Kiama Beach is 0.7 m (as determined from plots of frequency distributions in OAK 1981). This boulder size is entrained when the deep-water significant wave height exceeds 4.25 m (Figure 6).

It is interpreted that when wave heights exceed 4 m a competent energy level is reached at which point 90% of the available boulders have the potential to be transported. This size range only becomes mobile during storms where,  $H_s > \sim 4$  m and it is here where the estimates of threshold mass from equation (45) more closely match the field data as would

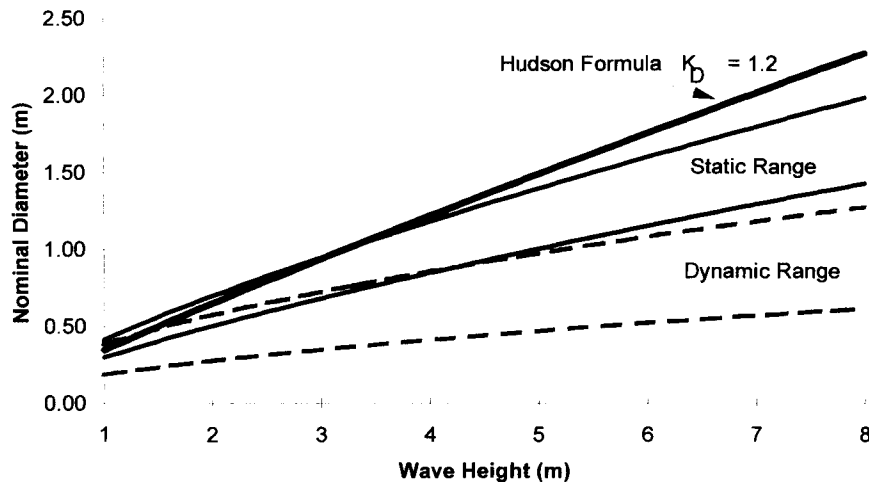


Figure 7. Comparison of the Hudson formula (1) with estimates from threshold equation (45) and the static equation (46) over a range of wave periods from 5 to 15 seconds.

be expected (Figure 6). At this high energy regime nearly all boulders composing the beach have the potential for entrainment, and therefore, friction and interlocking between boulders is greatly reduced.

#### Critical Threshold Versus Minimum Stability

Equation (45) provides a means for estimating threshold boulder mass for a set of given wave parameters and beach slope. Equation (46) is similar in that it estimates the minimum stone mass that is stable against movement. The important implication of having two separate equations is that two distinct boulder sizes are estimated and both are a function of wave period (Figure 7). This is very advantageous from a design perspective given that a range of wave periods for a design wave height can be used to estimate a size range of quarry material. In comparison, the Hudson Formula (equation 1) does not incorporate wave period, and hence, only a single size quarry stone is estimated. This is coupled with the fact that stability of the structure is dependent on choosing the proper stability coefficient and building the structure relative to the assumptions that represent a particular coefficient value (*i.e.* special placement is completed rather than random dumping).

One would expect that the difference between the estimated threshold mass (equation 45) and stable mass (equation 46) should be small. A comparison of estimates for these two equations shows that the difference is indeed small (Figure 7). The static range is slightly narrower than the dynamic range, a function of the role wave period and run-up plays in each of the equations (45) and (46). The estimated mass from equation (45) is dominated by the cube of wave run-up which in turn is a function of wave period. In contrast, the mass estimate from equation (46) is driven predominantly by the square of the breaker height.

Plotting two lines for the Hudson formula in Figure 8 with  $K_D$  values of 1.2 and 7 respectively estimates a tested static

range in stone mass relative to a range of wave heights. The value 1.2 is valid for sloping rock structures built with smooth rounded stones and the value of 7 is valid for placed rough angular stones (Table 7-8 SPM, 1984). Together they result in a Hudson stability range dependent on a difference in particle interlocking (Figure 8). Estimates from the stability equation (46) for wave periods of 5, 10 and 15 seconds respectively, plot within the stability range of the Hudson formula (Figure 8). Results show that increasing the wave period increases the estimated mass necessary to maintain stability.

Comparing the two equations in this fashion shows that equation (46) can indeed be considered a static equation, given that estimates lie in or above the static range of the Hudson formula (Figure 8). This result is advantageous in that with equation (46) wave period effects can be addressed when estimating a range of boulder sizes for a static shore-protection structure. The advantage also comes from not having to assume the proper  $K_s$  stability coefficient, as compared with the Hudson Formula (1) where the proper  $K_D$  value depends on estimating angularity of the structure material, mode of placement, morphology (*i.e.* structure head or trunk) and the expected form of wave breaking.

#### CONCLUSIONS

The two formulas derived could be useful in the initial evaluation and design of both static and dynamic revetments constructed with unconsolidated quarry stone. These equations offer a significant improvement over the Hudson formula. Equation (45) was derived to estimate the critical threshold mass,  $M_{Ru}$

$$M_{Ru} = \frac{\rho_s f_{BF} U_{max} R_u^3 2f}{K_r \left( \frac{\rho_s - \rho_w}{\rho_w} \right) g \tan \theta} \quad (45)$$

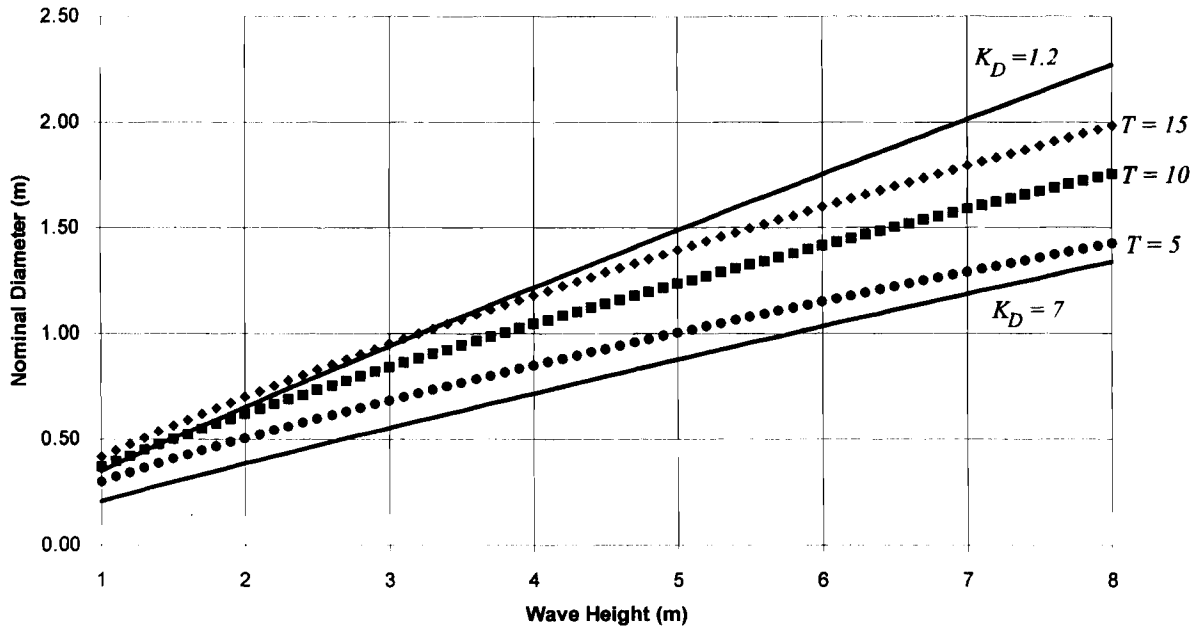


Figure 8. Comparison of estimates from the Hudson formula (1) and the stability equation (46) over a range in wave heights.

With substitution of  $H_{sb}$  for the length scale in the wave force expression (34) yields

$$M_{H_{sb}} = \frac{\rho_s f_{BF} U_{max} R_u H_{sb}^2 2f}{K_r \left( \frac{\rho_s - \rho_w}{\rho_w} \right) g \tan \theta} \quad (46)$$

where  $M_{H_{sb}}$  is the minimum stable mass. Equation (45) closely approximates the field data of the maximum entrained boulder at wave heights greater than 4 m (Figure 6). This “wave competency” level of 4.25 m entrains the measured  $D_{90}$  grain size fraction (the grain size fraction at which 90% of the beach material is smaller) for Kiama Beach. The interpretation is that under storm conditions boulder interlocking and friction are second order factors relative to swash velocity, run-up elevation, wave height and period. It can also be interpreted from figure six that boulder size, shape and packing dominate wave forces at less energetic wave conditions. If the beach were composed of uniform spheres a better prediction would be expected just as demonstrated in the flume studies of threshold entrainment under unidirectional currents. Furthermore, empirical testing of the  $K_r$  coefficient would also provide improved results for wave conditions below the wave competence level of the beach.

Increasing wave period will have the effect of transporting larger boulders due to increased wave power. Estimates from equation (45) when compared with field data (Figure 6) and equation (46) when compared to a range of wave heights and periods (Figures 7 & 8), support this conclusion. The advantage of equation (46) over the Hudson formula (1) is that it estimates unit mass in the static range without the need to estimate the value of a stability coefficient,  $K_r$ , which was set to one in all evaluations. Another advantage is that both (45)

and (46) estimate a range of rock sizes appropriate for design by varying the wave period rather than a single size. Moreover, both equations (45) and (46) incorporate the important physical parameters acting on the beach face: breaking wave height, wave period, swash velocity and elevation of the swash run-up, as opposed to relying on an empirical fit with offshore wave conditions.

However, a number of concerns for caution do exist! First and foremost are the number of components in the model that may have large uncertainty. In particular, estimating run-up is dependent on determining beach slope which can be problematic and vary widely even across short stretches of a boulder beach. Estimating maximum swash velocity is dependent on knowledge of breaker height and water depth. The friction factor,  $f_{BF}$ , even though objectively determined, does depend on roughness (grain-size dependent) and boundary layer thickness in the swash approximated by run-up height and an arbitrary estimator,  $D_{50}$ , of boulder size. These substitutions severely violate the underpinning assumptions in equation (15) which were developed for uniform steady flow with assumptions of a log-velocity profile. Therefore, at this point it is not fully demonstrated that the good fit of equation (45) with field data at wave heights above 4.25 m (Figure 6) is not fortuitous.

From an engineering design perspective each of the components can be defined for the equations. Indeed, estimating beach slope, breaker height and water depth at the toe of the structure are common practice (SPM, 1984). The use of the  $D_{50}$  size class in determining roughness is widely accepted when friction estimates for gravel transport in rivers are necessary. Values for the run-up attenuation coefficients,  $C_r$ , do exist and are the best estimates we have do date. Perhaps

the strongest support for further examination of these equations comes from Figure 8. The two solid lines are for the extremes in stability as supported by decades of wave tank experimentation to determine proper values for the stability coefficient,  $K_D$ , used in the Hudson formula. The biggest concern with the Hudson formula is that instability can result due to wave period effects. Equation (46) incorporates wave period and indeed the stability range inherent in increasing wave period is well demonstrated and falls within the Hudson limits (Figure 8). Using equations (45) and (46) as a check against estimates from the Hudson formula over a range of wave periods would be a prudent design step. Furthermore, if designing a dynamic revetment was the goal, then both equations would allow one to vary the physical variables that act on the beach face to test the predicted stability of a quarrystone source containing a mixture of sizes and shapes rather than arbitrarily picking stability coefficient values and assuming a single size quarry stone for construction. Clearly, future testing against field and wave tank data are necessary to fully evaluate the potential of the derived equations.

### ACKNOWLEDGMENTS

This work was funded in part through a fellowship provided to the author by the College of Oceanography and Atmospheric Sciences at Oregon State University while a graduate student. I would like to thank Dr. Small for making that fellowship possible. Many thanks go to Drs. Peter Klingeman and Rob Holman for all their help and advise. Dr. Charles Sollitt also provided useful review comments. Thanks goes Dr. Peter Howd for his reviews and encouragement early on in the development of this paper. Special thanks go to Nathaniel Plant (now Dr. Plant) and Kevin Tillotson for their friendship, review comments, encouragement and many games of hoops while trying to finish things up. I would also like to thank Dr. Don Forbes for his insightful review comments as journal referee. The author gratefully acknowledges the support and comments of the above individuals, however, all assumptions in the derivations or errors in interpretations are entirely my own.

### LITERATURE CITED

- AHRENS, J. and McCARTNEY, B.L., 1975. Wave period effect on the stability of riprap. *Proc. Civil Engr. in the Oceans/III*, American Society of Civil Engineers pp. 1019-1034.
- AHRENS, J.P., 1981. Irregular wave runup on smooth slope. *Tech. Aid No. 81-17*, Coastal Engineering Research Center, Waterways Experiment Station, Vicksburg, Miss.
- ALLSOP, N.W.H.; FRANCO, L., and HAWKES, P.J. 1985. Wave run-up on steep slopes - a literature review. *Report NO. SR 1*, Hydraulic Research, Wallingford U.K.
- BAGNOLD, R.A., 1940. Beach formation by waves: some model experiments in a wave tank. *Jour. Inst. C.E.*, 15, 27-52.
- BATTJES, A.J., 1974a. Surf Similarity. *Proc. 14th Conf. Coastal Eng. (ASCE)*, pp. 466-480.
- BATTJES, A.J., 1974b. Computation of set-up, longshore currents, run-up and overtopping on steep-slopes due to wind-generated waves. *Report 74-2*. Committee on Hydraulics, Dept. of Civil Engineering, Delft Univ. of Technology, Delft, the Netherlands.
- BRUUN, P. and GUNBAK, A.R., 1977. Stability of sloping structures in relation to  $\xi = \tan \alpha / \sqrt{H/L_0}$  risk criteria in design. *Coastal Engineering*, 1, 287-322.
- DALRYMPLE, R.A., 1992. Prediction of storm/normal beach profiles, *Jour. of Waterway Port, Coast and Ocean Eng.*, 118, pp. 193-200.
- HENDERSON, F.M., 1966. *Open Channel Flow* New York: MacMillan. 522p.
- HOLMAN, R.A., 1986. Extreme value statistics for wave run-up on a natural beach. *Coastal Engineering*, 9, 527-544.
- HUDSON, R.Y., 1952. Wave forces on breakwaters. *Transactions of the American Society of Civil Engineers (ASCE)*, 118, 653-685.
- HUGHES, M.G., 1995. Friction Factors for Wave Uprush. *Journal of Coastal Research*, 11(4), 1089-1098.
- HUNT, I.A., 1959. Design of seawalls and breakwaters. *Proc. ASCE*, 85, pp. 123-152.
- IRIBARREN, R., 1938. Una formula para el calculo de los discos de escollera. *Revista de Obras Publicas, Madrid* (A formula for the calculation of rock-fill dykes, translated by D. Heinrick, University of California, Dept. of Engineering T.R.-He-116-295 Berkeley, 1948.
- JOHNSON, C.N., 1987. Rubble beaches versus revetments. *Proc. Coastal Sediments '87 (ASCE)*, 2, 1217-1231.
- KOBAYASHI, N. and DESILVA, G., 1989. Wave transformation and swash oscillation on gentle and steep slopes. *Journal of Geophysical Research* 94 C1, 951-966.
- KOBAYASHI, N.; STRZELECKI, M.S., and WURJANTO, A., 1988. Swash oscillation and resulting sediment movement. *Coastal Engineering*, 12, 1167-1181.
- KOBAYASHI, N. and GREENWALD, J.H., 1986. Prediction of wave run-up and riprap stability. *Coastal Engineering*, 10, 1958-1971.
- KOMAR, P.D., 1998. *Beach Processes and Sedimentation*. Englewood Cliffs, NJ: Prentice-Hall, 429p.
- KOMAR, P.D. and GAUGHAN, M.K. 1973. Airy wave theory and breaker height prediction. *Proc. 13th Conf. Coastal Eng.*, 1, 405-418.
- LORANG, M.S., 1991. An artificial perched-gravel beach as a shore protection structure. *Proc. Coastal Sediments '91 (ASCE)*, 2, 1916-1925.
- NICHOLLS, R.J., 1988. Profile characteristics of shingle beaches. *Proc. 2nd European Workshop on Coastal Zones*. (Loutraki, Greece), Dept. of Civil Engr. National Technical University, Athens Greece.
- NICHOLLS, R.J., 1990. Managing erosion problems on shingle beaches: Examples from Britain. *3rd European Workshop on Coastal Zones*, (Paralimni, Cyprus), pp. 1-22.
- NOVAK, I.D., 1969. Swash-zone competency of gravel sediment. *Marine Geology*, 335-345.
- OAK, H.L., 1981. Boulder beaches: A sedimentological study. Ph.D. Thesis, Macquarie University, School of Earth Sciences, p. 272.
- OAK, H.L., 1985. Process inference from coastal-protection structures of boulder beaches. *Geogr. Ann.* 68, 25-31.
- PILARCZYK, K.W. and DER BOER, K., 1983. Stability and profile development of coarse materials and their application in coastal engineering. *Report No. 293, Delft Hydraulics Laboratory*.
- POWELL, K.A., 1988. The dynamic response of shingle beaches to random waves. *Coastal Engineering*, 12, 1763-1773.
- U.S. ARMY CORPS OF ENGINEERS, *Shore Protection Manual (SPM)*, 1984. 4th ed. 2 vols. Coastal Engineering Research Center, Waterways Experiment Station, Vicksburg, Miss, Govt. Printing Office, Washington, D.C.
- SILVESTER, R. and HSU, J.R.C., 1993. *Coastal Stabilization: Innovative Concepts*. Englewood Cliffs, NJ: Prentice-Hall, 578p.
- STERNBERG, R.W., 1972. Predicting Initial Motion and Bedload Transport of Sediment Particles in the Shallow Marine Environment. In: Swift, D.J.P. et al. editors. *Shelf Sediment Transport*, pp. 62-82.
- VAN DER MEER J.W., 1992. Stability of the seaward slope of berm breakwaters. *Coastal Engineering*, 16, 205-234.
- VAN DER MEER J.W., 1988. Rock slopes and gravel beaches under wave attack. *Delft Hydr. Communication*, No. 396.
- VAN DER MEER J.W., 1987. Stability of Breakwater Armour Layers-Design Formulae. *Coastal Engineering*, 11, 219-239.
- VAN DER MEER J.W. and PILARCZYK, K.W., 1986. Dynamic stability of rock slopes and gavel beaches. *Proc. 20th Coastal Engineering (ASCE)*, 2, 1713-1726.
- VAN DER MEER, J.W. and STAM, C.M., 1992. Wave run-up on

- smooth and Rock Slopes of Coastal Structures. *Jour. of Waterway Port. Coast and Ocean Eng.* 118, 534-550.
- VAN RIJN, L.C., 1982. Equivalent roughness of an alluvial bed. *Journal of the Hydraulics division (ASCE)*, HY10, 12-15-1218.
- WAAL, J.P. and VAN DER MEER, J.W., 1992. Wave Runup and Over-topping on Coastal Structures. *Coastal Engineering*, 16, 1758-1771.
- YALIN, M.S. and KARAHAN, E., 1979. Inception of sediment transport: *Jour. of the Hydraulics Division, Amer. Soc. Civil Engrs.*, 105, (HY11), 1433-1443.